A gain-of-function mutation in *ftsA* bypasses the requirement for the essential cell division gene *zipA* in *Escherichia coli*

Brett Geissler, Dany Elraheb, and William Margolin†

Department of Microbiology and Molecular Genetics, University of Texas Medical School, 6431 Fannin Street, Houston, TX 77030

Edited by Richard M. Losick, Harvard University, Cambridge, MA, and approved January 22, 2003 (received for review August 19, 2002)

ZipA and FtsA are recruited independently to the FtsZ cytokinetic ring (Z ring) and are essential for cell division of *Escherichia coli*. The molecular role of FtsA in cell division is unknown; however, ZipA is thought to stabilize the Z ring, anchor it to the membrane, and recruit downstream cell division proteins. Here we demonstrate that the requirement for ZipA can be bypassed completely by a single alteration in a conserved residue of FtsA (FtsA*). Cells with *ftsA in single copy in place of WT *ftsA* or with *ftsA** alone on a multicopy plasmid divide mostly normally, whether they are *zipA*+ or *zipA*−. Experiments with *ftsQAZ* and *ftsQA*Z* on multicopy plasmids indicate that *ftsQAZ*/*zipA*+ and *ftsQA*Z*/*zipA*− cells divide fairly normally, whereas *ftsQAZ*/*zipA*− cells divide poorly and *ftsQA*Z*/*zipA*+ cells display a phenotype that suggests their septa are unusually stable. In support of the idea that *ftsA** stabilizes Z rings, single-copy *ftsA** confers resistance to excess MinC, which destabilizes Z rings. The inhibitory effect of excess ZipA on division is also suppressed by *ftsA**. These results suggest that the molecular mechanism of the FtsA* bypass is to stabilize FtsZ assembly via a parallel pathway and that FtsA* can replace the multiple functions of ZipA. This is an example of a complete functional replacement of an essential prokaryotic cell division protein by another and may explain why most bacteria can divide without an obvious ZipA homolog.**

Cell division in *Escherichia coli* requires a number of conserved essential proteins. The earliest protein to arrive at the division site is FtsZ, which polymerizes to form the Z ring (1, 2). FtsA, ZipA, FtsK, FtsQ, FtsL, YgbQ, FtsW, FtsI, and FtsN are then recruited to the Z ring in sequential order (3–6). ZipA and FtsA localize to the Z ring independently (7, 8), whereas FtsL and YgbQ localization is codependent (3). The colocalization of all of these proteins presumably reflects the assembly of a protein machine at the membrane that orchestrates the growth of the division septum. FtsZ and FtsA are cytoplasmic proteins, and ZipA has a cytoplasmic C terminus and a membrane-bound N terminus (9). The others are integral membrane proteins with extensive periplasmic domains. Some key questions in bacterial cell division are how does this membrane-spanning machine assemble and how many subassemblies exist. Because FtsZ, FtsA, and ZipA all are required for recruitment of the later proteins (10, 11), understanding how these three proteins interact will shed light on the assembly of the entire machine.

ZipA was originally found in a biochemical screen for FtsZ-binding proteins (9) and has several proposed functions, one of which is to bundle FtsZ protofilaments *in vitro* (12, 13). This interaction between ZipA and FtsZ is mediated via the C termini of both proteins (14–16) and the bundling observed *in vitro* may translate into increased Z-ring stability *in vivo* (10, 12). Another proposed function of ZipA is to serve as a membrane anchor for the Z ring (17). This anchor function may be essential, because substitution of another domain with similar topology for the ZipA N-terminal membrane domain did not restore ZipA function (13). The third proposed function for ZipA is the recruitment of downstream proteins, as mentioned above.

FtsA is structurally similar to actin and other members of the ATPase superfamily (18). FtsA, like ZipA, interacts with the C terminus of FtsZ (14, 15, 19, 20), but its function in cell division is unknown. FtsA lacks a membrane-spanning domain but is membrane-associated (21, 22). Whereas Z rings assemble proficiently in the absence of either FtsA or ZipA, Z rings fail to form if both are absent (10). Therefore, it appears that FtsA and ZipA have overlapping roles, both in recruitment of downstream proteins and stabilizing the Z ring. The relative stoichiometry of FtsZ, ZipA, and FtsA is ≈150:10:1, which is crucial for cell division. For example, excess FtsA or ZipA inhibits cell division unless there is a corresponding increase in FtsZ (9, 23, 24). Interestingly, *Bacillus subtilis* lacks an obvious ZipA homolog, and FtsA is far more abundant, with the FtsZ/FtsA ratio at 5:1 (25).

Why is ZipA so crucial for *E. coli* cell division, yet apparently absent in most species outside the enteric bacteria (4)? One possibility is that other proteins fulfill the same role. Another is that FtsA, which is much more widely conserved, might be able to substitute for ZipA if FtsA were at a higher concentration or in a different conformation. This idea prompted us to test whether *E. coli* could find a way to survive without ZipA. Our hypothesis was that if most bacteria can divide without ZipA, then there might be a way to bypass the need for it in *E. coli* and that this bypass pathway might shed important light on the functions of FtsA, ZipA, and FtsZ. Here, we show that cell division in *E. coli* can indeed occur without ZipA, provided there is a corresponding change in the function of FtsA.

Materials and Methods

Media, Chemicals, and Other Reagents. Antibiotics were added to LB medium at the following concentrations: 40–50 μg/ml kanamycin (kan), 20 μg/ml chloramphenicol, 50 μg/ml ampicillin, 50 μg/ml spectinomycin (spc), and 10 μg/ml tetracycline. L-Arabinose and isopropyl-β-D-galactopyranoside (IPTG) were added at the concentrations indicated in the text. M9 glucose medium and LB medium have been described (26). Protein markers were from Invitrogen.

Strains and Plasmids. *E. coli* host strains for physiological experiments include TX3772 [MG1655 *lacU169* (27)], WM1115 [*ftsA12* (Ts) in TX3722], and WM1282 (see below). For further details of all strains and plasmids see Table 2, which is published as supporting information on the PNAS web site, www.pnas.org. The *ftsAZ* region from a Δ*zipA* suppressor strain (WM1520) was first cloned by replacing the *Bgl*II–*Cla*I fragment in pZAQ (28) with the corresponding genomic fragment from WM1520 by PCR. The resulting plasmid was called pZAQsup, then pZA*Q once the mutation in *ftsA* was confirmed to be the suppressor. Plasmid pET28-FtsA was made by cloning *ftsA* into *Nde*I–

This paper was submitted directly (Track II) to the PNAS office.

Abbreviations: kan, kanamycin; spc, spectinomycin; IPTG, isopropyl-β-D-galactopyranoside.

†To whom correspondence should be addressed. E-mail: William.Margolin@uth.tmc.edu.

*Bam*HI-digested pET28a (Novagen); the *Nde*I site contains the *ftsA* start codon. Plasmid pET28-FtsA* was made by replacing an internal *Kpn*I–*Asc*I fragment with the *Kpn*I–*Asc*I fragment from pZA*Q. *Xba*I–*Pst*I fragments of pET28a-FtsA and pET28a-FtsA* containing *ftsA* fused to the hexahistidine tag were then cloned into *Xba*I–*Pst*I-digested pBAD33 (29), creating pBAD-FtsA and pBAD-FtsA*, respectively. To create an IPTG-inducible *zipA*-GFP fusion (pWM796), the *zipA* gene lacking a stop codon was PCR-amplified and cloned as a *Sac*I–*Xba*I fragment to replace *ftsZ* in pZG (15). Plasmid pWM1703 was made by filling in the *Xba*I site of pWM796, thus introducing a stop codon after *zipA*. Plasmid pWM1802 expresses ZipA from the P*trc* promoter of pDSW208 (30). To construct the IPTG-inducible *minC* expression plasmid pWM1509, *minC* was cloned into the *Xba*I site of pDSW209 (30) to make a GFP-*minC* fusion. To make a GFP-FtsN fusion, *ftsN* was cloned between the *Sac*I and *Xba*I sites of pDSW207 (30).

Isolation and Mapping of *ftsA* R286W. The ZipA depletion strain containing Δ*zipA*::*aph* and a temperature-sensitive plasmid carrying *zipA* and *ftsZ* (CH5/pCH32) was obtained from Piet de Boer (Case Western Reserve University, Cleveland) and has been described (9). We renamed this strain WM1282. To isolate suppressors of the *zipA* null mutation, WM1282 cells were grown at 28°C in LB kan to early logarithmic phase, then shifted to 42°C, diluted once, and incubated at 42°C for 3 days. After allowing for settling of the long filaments, a small aliquot from the top was removed and plated on prewarmed LB kan plates at 42°C. Four colonies appeared, which were purified on LB kan and LB spc at 42°C. The loss of the temperature-sensitive *zipA* covering plasmid pCH32 was confirmed by the lack of growth on LB spc. P1 phage lysates were made from all four survivor strains as well as WM1282 and used to transduce TX3772 (WT) or TX3772 containing pCH32 (WM1302) to Kan^R at 32°C. All five of the lysates resulted in 50–100 Kan^R transductants with TX3772/pCH32 recipients but no transductants with TX3772 recipients, indicating that the suppressor was not linked to Δ*zipA*::*aph*.

To determine linkage to *ftsAZ*, WM1302 was transduced to $tetracycline^R$ at 30°C with a P1 phage lysate from a *leu*::Tn*10* strain, WM1109. The Leu− phenotype was verified by the failure of the cells to grow on M9 glucose plates lacking leucine. WM1302 *leu*::Tn*10* was then transduced to kan^R at 30°C with a phage P1 lysate from WM1282, introducing Δ*zipA*::*aph* into the chromosome and making the cells thermosensitive. This strain in turn was then transduced to Leu^+ (growth on M9 glucose plates) with a P1 lysate made from the Δ*zipA* suppressor strain WM1520. This process allowed ≈50% cotransduction of the *ftsQAZ* region, and thus the suppressor, into this strain. One of the many transductants able to form colonies at 42°C was saved and grown further at 42°C to remove pCH32; it was then confirmed to be Spc^S. WM1659 (*ftsA**) was constructed by transducing WM1109 (TX3772 *leu*::Tn*10*) to Leu^+ with a P1 lysate from WM1520. This process allowed cotransduction of *ftsA** into this strain at ≈50% efficiency. WM1659 was then transduced to Kan^R with the Δ*zipA*::*aph* allele from WM1282 to make WM1657.

Antibody Production and Immunoblot Analysis. To obtain anti-ZipA antiserum, we purified the C-terminal cytoplasmic domain of ZipA as was done in ref. 13. This segment of *zipA*, corresponding to residues 186–328, was cloned between the *Bam*HI and *Xho*I sites of pET28a+ to create pWM1610. This plasmid carries the *zipA* segment fused to T7 and hexahistidine tags at the N terminus and a hexahistidine tag at the C terminus [HT-ZipA(186–328)-H]. The ≈18.4-kDa HT-ZipA(186–328)-H protein was expressed in BL21(λDE3)/p*lysS* cells carrying pWM1610 after induction with 1 mM IPTG for 3 h and affinity purification as described (13). The purified protein was used to raise rabbit anti-ZipA polyclonal antiserum (Capralogics, Hardwick, MA). To detect GFP-MinC and FtsZ, we used affinity-purified polyclonal anti-GFP and anti-FtsZ, as described (27). For immunoblot analysis, 15 μg of total protein from each sample was separated by SDS/PAGE and transferred to a nitrocellulose membrane. The membrane was blocked with gelatin and probed with primary antibody (1:5,000 for anti-ZipA) followed by goat-anti-rabbit-conjugated horseradish peroxidase secondary antibody, and developed with ECL reagents (Amersham Pharmacia). A Fluorichem Imager was used to quantitate the chemiluminescence of the resulting protein bands.

Microscopy and Analysis of Cells. In most cases, phase-contrast images were taken of wet mounts of cells. For determination of cell lengths, cells were fixed on coverslips before microscopic analysis. Immunofluorescence microscopy with anti-FtsZ antibody was performed as described (27). Cell lengths were measured with PHOTOSHOP (Adobe Systems, Mountain View, CA) and statistics were compiled in EXCEL (Microsoft). Growth rates were followed by optical density with a Klett–Summerson photometer. Viable counts were determined by counting the number of colonies after plating dilutions of cells on LB agar.

Molecular Modeling and Protein Alignments. The FtsA crystal structure was imported from the Protein Data Bank and manipulated graphically with WEBLAB VIEWERLITE 3.20 (Molecular Simulations, Waltham, MA). Protein alignments were obtained by using BLASTP at the National Center for Biotechnology Information web site (www.ncbi.nlm.nih.gov), and then optimized manually.

Results and Discussion

Isolation of Suppressors of a *zipA* Null Mutant. Because ZipA is not highly conserved, we hypothesized that it might be possible to isolate mutants of *E. coli* that could bypass the requirement for ZipA in cell division. To select for such mutants, we used WM1282, a recombination-deficient strain harboring a Δ*zipA*::*aph* (Kan^R) disruption and a Spc^R *zipA*-containing plasmid (pCH32) that is thermosensitive for replication (9). The cells were grown at 30°C and then shifted to 42°C for many generations to promote loss of the plasmid and select for suppressors. Plating at 42°C yielded four Spc^S Kan^R colonies that lacked the *zipA*-covering plasmid. All four of these strains, which may have been siblings as they were from the same culture, were able to transfer Kan^R via P1 transduction to a WT recipient strain carrying pCH32 but not to a strain lacking the plasmid, suggesting that Δ*zipA*::*aph* was still intact in these survivor strains and that the suppressor was not located within cotransduction distance. The presence of the chromosomal Δ*zipA*::*aph* disruption was confirmed by PCR, sequencing, and Southern blotting (data not shown). These results suggested that we had isolated one or more extragenic suppressor mutations that could bypass the requirement for *zipA*.

The absence of detectable ZipA protein in the Δ*zipA*::*aph* suppressor strains was confirmed by immunoblotting with an antibody raised against a C-terminal domain of ZipA (Fig. 1, lane 3, and data not shown). As has been observed (9), ZipA protein migrated with an apparent molecular mass of ≈50 kDa despite its predicted size of 36.5 kDa (Fig. 1, lane 1). Specificity of our antibody for ZipA was demonstrated in three ways. First, overproduction of ZipA resulted in a more intense 50-kDa band compared with the control (Fig. 1, lane 4, compare with lane 1). Second, overproduction of ZipA-GFP resulted in a new band at ≈80 kDa, the predicted size of the 50-kDa ZipA fused to 27-kDa GFP (Fig. 1, lanes 2 and 5). Third, the 50-kDa band became significantly less intense after depletion of ZipA by growth of WM1282 at 42°C for 4 h (Fig. 1, compare lanes 6 and 7).

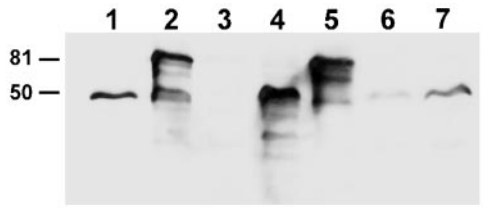

Fig. 1. Immunoblot showing cellular ZipA in strains used in this study. Lane 1, TX3772 (WT); lane 2, pWM796 (ZipA-GFP) in WM1659 (*ftsA**) + 1 mM IPTG; lane 3, WM1657 (*ftsA** Δ*zipA*); lane 4, pWM1703 (ZipA) in WM1657 (*ftsA** Δ*zipA*) + 1 mM IPTG; lane 5, pWM796 (ZipA-GFP) in WM1657 (*ftsA** Δ*zipA*) + 1 mM IPTG; lane 6, WM1282 grown at 42°C for 4 h to deplete ZipA; lane 7, WM1282 grown at 30°C. *ftsA** is the suppressor allele. Positions of 50-and 81-kDa protein markers are shown on the left.

A Single Residue Change in FtsA Is Necessary to Confer ZipA Independence. Because ZipA, FtsA, and FtsZ are known to interact, we reasoned that the suppressor mutations might map to the *ftsAZ* region. To determine linkage to *ftsAZ*, we used a recipient strain for phage P1 transduction that contained a *leu*::Tn*10* marker, which is ≈50% linked to *ftsZ* by cotransduction, Δ*zipA*::*aph* from WM1282, and the thermosensitive *zipA*-covering plasmid (pCH32). Using one of the Δ*zipA*::*aph* suppressor strains (WM1520) as a donor, this thermosensitive recipient was transduced to Leu+. Approximately 50% of the transductants became thermoresistant, suggesting that the *zipA* suppressor mutation was successfully cotransduced and that it mapped in or near *ftsAZ*.

To verify that the suppressor was in *ftsAZ* and to map it more precisely, we PCR-amplified a *Bgl*II–*Cla*I fragment containing most of *ftsA* and all of *ftsZ* from the original suppressor strain WM1520 and replaced the native *ftsAZ* in pZAQ with these *ftsAZ* sequences. WT TX3772 cells containing this new plasmid (pZAQsup) or the original pZAQ were then transduced with Δ*zipA*::*aph*. Surprisingly, Kan^R colonies were isolated at a similar frequency in both recipient strains (see below). However, pZAQ-containing cells were highly filamentous, whereas the pZAQsup-containing cells were short (see below). Therefore, the suppressor mapped to the *ftsAZ* region downstream from the *Bgl*II site in *ftsA*. DNA sequencing of the entire *ftsAZ* region containing the suppressor revealed a single base change from the WT sequence, a C → T transition at base pair 856 of *ftsA*, corresponding to an arginine-to-tryptophan change at position 286 in the FtsA protein. All four original suppressor strains contained the same mutation, which we will refer to hereafter as *ftsA**. Likewise, pZAQsup was renamed pZA*Q. R286W may be the only *ftsA* mutation that can cause the bypass, because when we deleted *zipA* by an independent method and selected independent surviving colonies, all of those tested contained the R286W change (B.G. and W.M., unpublished results).

Mostly Normal Cell Division in Cells Containing *ftsA in Place of WT *ftsA*.** Although *ftsA** allowed survival of Δ*zipA* cells, we were interested to know what effects *ftsA**, either alone or with Δ*zipA*, had on cell division and growth. We constructed two derivatives of TX3772 that contained *ftsA** instead of native *ftsA*; one was *zipA*+ (WM1659) and the other Δ*zipA* (WM1657) (see *Materials and Methods*). The strains grew normally, as doubling times for TX3772, WM1659, and WM1657 in LB were 29, 30, and 31 min, respectively, at 37°C and 115, 111, and 111 min, respectively, at 28°C. Viable counts were very similar under both conditions. The morphology of most *ftsA** cells, whether *zipA*+ or *zipA*−, was similar to those of WT cells; the same was true for Z rings as examined by immunofluorescence (Fig. 2 *A–F*). The most notable differences were that (*i*) a small proportion of *ftsA** cells exhibited twisting at the septum that was made more visible after elongating the cells with cephalexin (Fig. 2 *G–J*), and (*ii*) some minicells were observed for WM1659 but not the others (data not shown). Minicells may arise because of the *ftsA**-mediated resistance to the MinC division inhibitor (see below). We conclude that the cell division deficiency of cells lacking ZipA is suppressed by *ftsA**, although cell division is not completely normal in cells with *ftsA**.

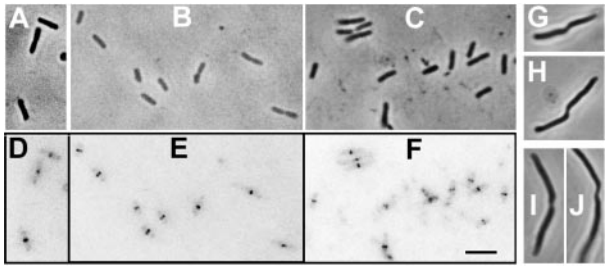

Fig. 2. Mostly normal cell division with *ftsA** replacing WT *ftsA*. Shown are WT strain TX3772 (*A* and *D*), *ftsA** *zipA*+ strain WM1659 (*B* and *E*), and *ftsA** Δ*zipA* strain WM1657 (*C* and *F*). (*A–C*) Phase-contrast images. (*D–F*) Immunofluorescence microscopy for FtsZ (black staining) of the cells in *A–C*, respectively. (*G–J*) Phase-contrast images of nondividing WM1657 cells after growth in cephalexin for 2 h to accentuate the twisting at the potential septum. (Scale bar = 5 μm.)

The *ftsA Mutation Is Sufficient to Bypass the Requirement for ZipA.** To confirm that mutations other than *ftsA** and coexpression of *ftsZ* or *ftsQ* were not necessary for ZipA-independent cell division, we introduced plasmids pBAD-FtsA and pBAD-FtsA* into a thermosensitive *ftsA* mutant (WM1115) and confirmed that either *ftsA* or *ftsA** could complement the mutant without addition of arabinose inducer. With arabinose, WT cells with either plasmid became filamentous, which is the expected FtsA oveproduction phenotype (23, 24). However, when the pBAD derivatives were introduced into the *zipA* depletion strain WM1282, only pBAD-FtsA* allowed colony formation at 42°C with or without arabinose (Fig. 3 and data not shown). As expected, WM1282 cells containing pBAD-FtsA became filamentous upon shifting to 42°C, whereas cells containing pBAD-FtsA* remained short (data not shown). Likewise, transduction of TX3772 containing pBAD-FtsA* with Δ*zipA*::*aph* yielded viable colonies but TX3772/pBAD-FtsA did not, either with or without arabinose (data not shown). We conclude from these data that synthesis of FtsA* alone, but not FtsA alone, is sufficient to bypass the requirement for ZipA, and that no secondary mutations are necessary. In support of this conclusion, FtsZ levels normalized to total cell protein as measured by Western blots were similar in *ftsA** and *ftsA*+ cells (data not shown), ruling out the possibility that *ftsA** mutation significantly increased *ftsZ* expression.

FtsA* Eliminates the Requirement for ZipA in Recruitment of Downstream Cell Division Proteins. The bypass of the ZipA requirement for cell division suggests that all functions of ZipA, including

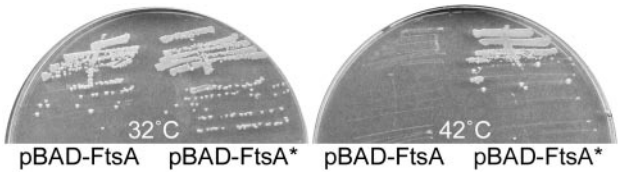

Fig. 3. FtsA* is sufficient to bypass the need for ZipA. Colony growth is shown at 32°C or 42°C on LB chloramphenicol plates without arabinose for the ZipA depletion (WM1282) strains containing the plasmids indicated.

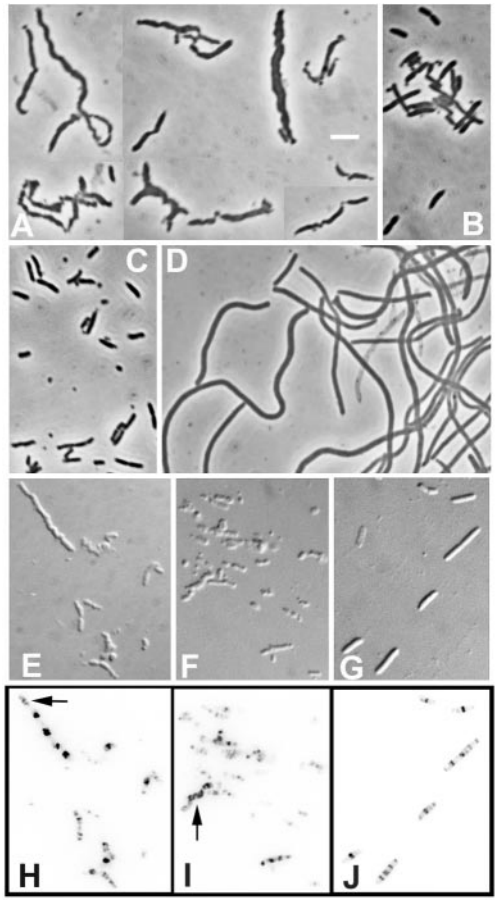

Fig. 4. Effects of overproduction of FtsA or FtsA* on cell morphology. (*A–D*) Representative phase-contrast images of pZA*Q in TX3772 (*A*), pZAQ in TX3772 (*B*), pZA*Q in TX3772 transduced with Δ*zipA*::*aph* (*C*), and pZAQ in TX3772 transduced with Δ*zipA*::*aph* (*D*). (*E–J*) Nomarski (*E–G*) and FtsZ immunofluorescence microscopy (*H–J*) of pZA*Q in TX3772 (*E*, *F*, *H*, and *I*) and pZAQ in TX3772 (*G* and *J*). Arrows in *H* and *I* highlight helical FtsZ patterns. (Scale bar = 5 μm.)

recruitment of later cell division proteins, are now taken care of by FtsA*. However, another possibility, albeit unlikely, was that in the presence of FtsA*, later cell division proteins were no longer recruited nor required for division. We addressed this question in two ways. First, when WM1657 and WM1659 cells were treated with cephalexin, which inhibits the late cell division protein FtsI, the cells became filamentous (Fig. 2 *G–J*). This finding indicates that FtsI remains essential. Second, a GFP fusion to the last known cell division protein recruited to the division site, FtsN, localized correctly to the division site independently of ZipA as long as FtsA* was present (data not shown). These results suggest that in the absence of ZipA the functions of later cell division proteins remain intact.

This conclusion has important implications for the assembly of the cell division protein complex. ZipA is required for recruitment of late cell division proteins (11). Our results indicate that it is unlikely that ZipA recruits these proteins directly, but instead normally acts via stimulation of recruitment by FtsZ, FtsA, or another as yet unknown factor.

Effects of Multicopy Coexpression of *ftsQA*Z* and *ftsQAZ*. Because *ftsA** does not appear to have a significant phenotype when in single copy other than some minicells and twisted septa with cephalexin, we investigated the effects on cell division when *ftsA** was expressed in multiple copy along with *ftsQ* and *ftsZ*. In *zipA*+ cells, plasmid pZAQ, which carries native *ftsQAZ* and some flanking sequences, produced a mixture of minicells and cells of mostly normal length in *zipA*+ cells (Fig. 4*B* and data not shown). This finding is consistent with previous reports (31, 32). In contrast, a significant proportion of cells containing pZA*Q (pZAQ with the single-residue change to make *ftsA**) displayed pronounced morphological abnormalities in *zipA*+ cells (Fig. 4*A*) whereas pZA*Q/*zipA*- cells looked much like pZAQ/*zipA*+ cells (Fig. 4*C*). More than half of pZA*Q/*zipA*+ cells exhibited twisted septa that were much more extensive than in cells with single-copy *ftsA**, abnormal polar morphology, cell chains, and other morphological aberrations. These results suggested that the septa might be abnormally stable, so FtsZ staining was examined by immunofluorescence microscopy. In contrast to pZAQ/*zipA*+ cells, which had Z rings at potential division sites and cell poles (Fig. 4 *G* and *J*), FtsZ staining in pZA*Q/*zipA*+ cells was much more irregular, varied greatly in intensity among cells, and often exhibited helical patterns (Fig. 4 *E*, *F*, *H*, and *I*, arrows in *H* and *I*). These results suggested that Z rings might be unusually stable in *zipA*+/pZA*Q cells, but we could not always correlate FtsZ staining with any particular type of morphological aberration. For example, some obvious twisted septa had FtsZ staining, but others had no detectable FtsZ staining, perhaps because the cells were already dead. The abnormal morphology was not observed with pZAQ (Fig. 4*C*) or after overproduction of FtsA or FtsA* alone (data not shown), suggesting that

Table 1. Resistance of *ftsA to division inhibition caused by excess ZipA or MinC**

Plasmid, + or − inducer for 2 h	Expressed protein	Relevant genotype	Relative protein level	Average cell length (length range) in μm	Relative viability
pWM1509	GFP-MinC	*ftsA** (WM1659)	1.0	1.4 (0.8–2.1) *n* = 44	1.0
pWM1509 + IPTG	GFP-MinC	*ftsA** (WM1659)	3.8	3.0 (1.0–6.5) *n* = 39	0.7
pWM1509	GFP-MinC	*ftsA*+ (TX3772)	1.1	3.6 (1.6–27.5) *n* = 44	0.3
pWM1509 + IPTG	GFP-MinC	*ftsA*+ (TX3772)	4.5	46.8 (3.3–87.3) *n* = 26	0.0003
pWM1802	ZipA	*ftsA** (WM1659)	1.0	2.8 (1.6–8.9) *n* = 64	1.0
pWM1802 + IPTG	ZipA	*ftsA** (WM1659)	2.4	3.0 (1.5–7.3) *n* = 118	0.6
pWM1802	ZipA	*ftsA*+ (TX3772)	1.0	2.9 (1.7–4.5) *n* = 63	0.9
pWM1802 + IPTG	ZipA	*ftsA*+ (TX3772)	2.0	21.0 (2.9–54.6) *n* = 145	0.1

Cells were at equivalent densities in LB at 37°C when 1 mM IPTG was added; cells were harvested 2 h later for analysis. The same cell samples were used for immunoblots, cell length measurements by microscopy, and viable colony counts. Cells were all at equivalent densities at the start of the experiment. Immunoblots were probed with either anti-GFP or anti-ZipA antibodies as appropriate; protein bands were from the same blot and therefore directly comparable. For the four samples in the GFP-MinC or ZipA experiment, the lowest amount of protein was normalized to 1. For cell length measurement in row 1, minicells were included, resulting in short average length. Relative viable counts were obtained by calculating colony-forming units after plating dilutions on LB agar at 37°C; the highest counts for each of the two experiments (MinC and ZipA) were normalized to 1. Results for pWM1703 were similar to those for pWM1802. *n* = Number of cells counted.

coexpression of *ftsQ* and/or *ftsZ* with *ftsA** in multicopy is required for the phenotype.

We found that pZAQ allowed growth of colonies transduced with Δ*zipA*::*aph*, although the cells were very filamentous (Fig. 4*D*). This finding suggested that perhaps overproduced WT FtsA could mimic the chromosomal *ftsA** allele and partially suppress the absence of *zipA*. However, as mentioned above, overproduction of FtsA by arabinose induction of pBAD-FtsA did not suppress *zipA*::*aph* or increase viability of WM1282 at 42°C. This result suggests that coexpression of *ftsQ* and/or *ftsZ* on pZAQ is probably necessary for this weak suppression.

FtsA* Suppresses Cell Division Inhibition Caused by Overproduction of MinC and ZipA. Overproduction of MinC destabilizes Z rings, resulting in cell filamentation (33). The potential stabilization of septa by excess FtsA* from pZA*Q (Fig. 4) prompted us to test whether Z rings in FtsA*-containing cells were more resistant to MinC than WT cells. We used a GFP-MinC fusion (pWM1509) because it has been shown to be functional (34) and we could use anti-GFP antibodies to quantitate its cellular levels. IPTG-mediated induction of GFP-MinC overproduction for 2 h from pWM1509 resulted in a 4-fold increase in GFP-MinC levels in TX3772 and WM1659 (Table 1 and Fig. 6, which is published as supporting information on the PNAS web site). As expected, induced TX3772 cells elongated >10-fold on average compared with uninduced cells (Table 1). In contrast, induced cells of the *ftsA** strain WM1659 were only twice as long as uninduced *ftsA** cells on average. GFP-MinC induction resulted in an ≈1,000-fold loss of viability of TX3772 cells, as compared with WM1659 overproducing GFP-MinC, uninduced TX3772, or uninduced WM1659 (Table 1).

Although Z-ring stability can be enhanced by doubling *zipA* gene dosage and possibly increasing ZipA protein level (12), overproduction of ZipA several-fold also inhibits cell division, which can be reversed by increasing FtsZ levels (9, 13). Because FtsA* renders ZipA unnecessary, we investigated whether FtsA* might confer resistance to the negative effects of excess ZipA. IPTG-mediated induction of ZipA overproduction from pWM1802 for 2 h in either TX3772 or WM1659 (*ftsA**) resulted in a 2-fold increase in ZipA levels over uninduced levels in either strain (Table 1 and Fig. 7, which is published as supporting information on the PNAS web site). WT TX3772 cells overproducing ZipA became highly filamentous, elongating 7-fold on average compared with uninduced cells. In contrast, WM1659 (*ftsA**) cells with 2-fold excess ZipA did not elongate at all compared with uninduced cells (Table 1). ZipA overproduction in TX3772 also resulted in ≈10-fold less viability as compared with induced WM1659 or uninduced TX3772 and WM1659 (Table 1). Similar results were obtained in experiments with pWM1703, another plasmid that expresses ZipA (data not shown). Previously, at least 6-fold higher levels of ZipA or several tagged and deletion derivatives of ZipA were needed to observe significant cell filamentation (13); however, our results with inhibition of cell division after only 2-fold overproduction of ZipA are reproducible and may result from differences in strain backgrounds or induction conditions.

These data demonstrate that the presence of *ftsA** resists cell division inhibition and killing caused by excess ZipA or MinC (see also Figs. 6 and 7). Whereas the mechanism by which excess ZipA inhibits septation is not clear, the MinC resistance of *ftsA** suggests that FtsA* acts to stabilize Z rings. Because overproduction of WT FtsA can suppress MinC-mediated cell filamentation (35), we suggest that *ftsA** may mimic overproduction of FtsA, at least for anti-MinC activity. Moreover, our results indicate that *ftsA** not only bypasses the requirement for ZipA, but also antagonizes the negative effects of excess ZipA.

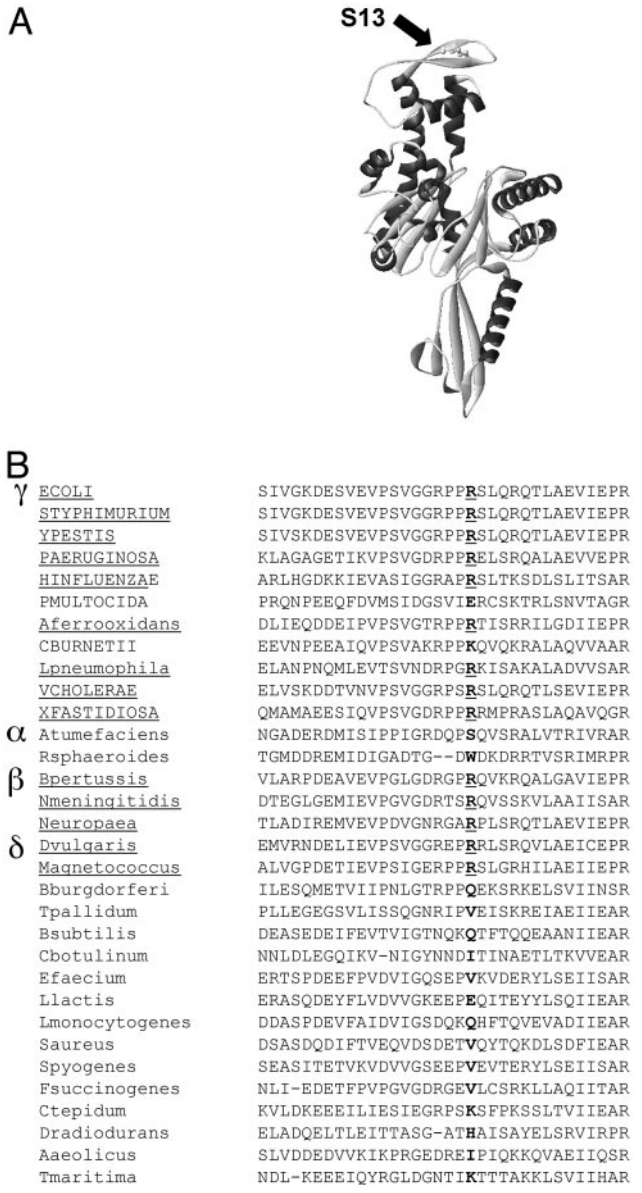

Fig. 5. Molecular modeling of FtsA* (R286W) on the FtsA crystal structure and conservation of R286 across species. (*A*) A ribbon diagram of FtsA from *T. maritima*, with K287 highlighted as a ball-and-stick representation within the S13 domain. (*B*) An amino acid alignment of the region surrounding the FtsA S13 β-sheet (IKTTT in *T. maritima*) based on the presence or absence of the conserved arginine. From the top down, the groupings are γ, α, β, and δ Gram-negative proteobacteria, other Gram-negative proteobacteria, Gram-positive bacteria, and the most divergent species. Species in all caps have ZipA homologs; species underlined have the conserved arginine.

Conservation of R286 and Its Proposed Location in the FtsA Molecule. An alignment of FtsA proteins shows that R286 is well conserved among the γ-proteobacteria, which is the same group of bacteria that contain ZipA homologs (Fig. 5*B*). Of the species known to have ZipA, all have arginine or lysine at this position except for *Pasteurella multocida*, which has a glutamate. However, many species lacking ZipA also often have arginine at this position. With one exception, tryptophan, phenylalanine, and tyrosine are absent at this position, ruling out the possibility that W286 is required for viability in species lacking a ZipA homolog.

Residue R286 of *E. coli* FtsA appears to be equivalent to K287 of *Thermotoga maritima* FtsA, which has been crystallized (Fig.

5*B*). K287 lies within the S13 β-sheet of subdomain 2B, at the top of the monomer structure (18) (Fig. 5*A*). This subdomain has high sequence conservation among FtsA homologs (Fig. 5*B*) and some conservation within other members of the actin family. However, the sequence similarity in this region between *E. coli* and *T. maritima* is too low to be certain of its precise position in the structure or whether R286 faces in or out of the *E. coli* FtsA protein. It is intriguing that (*i*) K287 in *T. maritima* can form a salt bridge with D250 within the same subunit (data not shown), and (*ii*) residues within the similar S13 loop of MreB, another actin family member, contact residues in helix H8 of the previous subunit during polymerization of MreB protofilaments (36). No similar salt bridge occurs in *E. coli* FtsA, as there are no acidic residues in the vicinity of the D250 equivalent. However, the MreB functional model suggests that perhaps the R286W change causes a significant alteration in the ability of FtsA monomers to self-interact (37). Another possibility is that this region is involved in contacting FtsZ and the R286W change alters the interaction. Clearly, future biochemical characterization of the FtsA and FtsA* proteins and their interactions with FtsZ is needed, as well as more information about the function of specific domains and residues in FtsA.

Implications for ZipA and FtsA Function. One possible explanation for why bacteria outside the γ-proteobacterial family apparently lack ZipA homologs is that they contain ZipA-like homologs too divergent to discern by sequence comparisons. However, it is also possible that these other species contain an FtsA with more FtsA*-like properties and/or have significantly higher intracellular concentrations of FtsA, therefore naturally bypassing the requirement for ZipA. The possibility that higher FtsA levels might be sufficient in some situations stems from our finding that elevated levels of WT FtsA from pZAQ can partially compensate for the lack of ZipA. *B. subtilis*, whose FtsA is present at significantly higher concentrations than that of *E. coli* (25), may be an example of this strategy.

Nevertheless, it remains surprising that in *E. coli ftsA** can bypass the need for ZipA without a significant cost. The normal growth and mostly normal cell division phenotype in the absence of ZipA indicates that FtsA* can perform all tasks attributable to ZipA, including protein recruitment, tethering FtsZ to the membrane, and stabilizing assembled FtsZ. These conclusions support the idea that ZipA primarily acts as an accessory factor that regulates FtsZ assembly. Other candidates for this type of accessory role are the nonessential *B. subtilis* proteins ZapA and EzrA, which positively and negatively modulate FtsZ assembly, respectively (38, 39). Interestingly, although EzrA and ZipA have opposing effects on FtsZ assembly, both have similar topology, with a cytoplasmic C terminus and a membrane-bound N terminus. It is likely that these accessory factors function to maintain a balance between FtsZ assembly and FtsZ disassembly, and that the added putative stabilization function of FtsA* just happens to compensate nearly perfectly for the loss of ZipA stabilization activity. Just as new factors involved in cell division are being discovered, our results here demonstrate that some factors may be found to be replaceable under the right conditions. This approach should help to define the roles of these factors in *E. coli* and diverse organisms and may also help to minimize the number of purified proteins needed for future *in vitro* studies of cell division.

We are grateful to Piet de Boer for the CH5/pCH32 (WM1282) ZipA depletion strain and David Weiss for PDSW207, PDSW208, and PDSW209. We thank Qin Sun, Xiaolan Ma, and Ryan Shields for constructing some of the plasmids used in this work and other lab members for helpful discussions. This study was supported by National Institutes of Health Grant R01-GM61074.

1. Bi, E. & Lutkenhaus, J. (1991) *Nature* **354,** 161–164.
2. Addinall, S. G. & Holland, B. (2002) *J. Mol. Biol.* **318,** 219–236.
3. Buddelmeijer, N., Judson, N., Boyd, D., Mekalanos, J. J. & Beckwith, J. (2002) *Proc. Natl. Acad. Sci. USA* **99,** 6316–6321.
4. Margolin, W. (2000) *FEMS Microbiol. Rev.* **24,** 531–548.
5. Mercer, K. L. & Weiss, D. S. (2002) *J. Bacteriol.* **184,** 904–912.
6. Chen, J. C. & Beckwith, J. (2001) *Mol. Microbiol.* **42,** 395–413.
7. Hale, C. A. & de Boer, P. A. (1999) *J. Bacteriol.* **181,** 167–176.
8. Liu, Z., Mukherjee, A. & Lutkenhaus, J. (1999) *Mol. Microbiol.* **31,** 1853–1861.
9. Hale, C. A. & de Boer, P. A. (1997) *Cell* **88,** 175–185.
10. Pichoff, S. & Lutkenhaus, J. (2002) *EMBO J.* **21,** 685–693.
11. Hale, C. A. & de Boer, P. A. (2002) *J. Bacteriol.* **184,** 2552–2556.
12. Raychaudhuri, D. (1999) *EMBO J.* **18,** 2372–2383.
13. Hale, C. A., Rhee, A. C. & de Boer, P. A. (2000) *J. Bacteriol.* **182,** 5153–5166.
14. Wang, X., Huang, J., Mukherjee, A., Cao, C. & Lutkenhaus, J. (1997) *J. Bacteriol.* **179,** 5551–5559.
15. Ma, X. & Margolin, W. (1999) *J. Bacteriol.* **181,** 7531–7544.
16. Haney, S. A., Glasfeld, E., Hale, C., Keeney, D., He, Z. & de Boer, P. (2001) *J. Biol. Chem.* **276,** 11980–11987.
17. Erickson, H. P. (2001) *Curr. Opin. Cell Biol.* **13,** 55–60.
18. van Den Ent, F. & Lowe, J. (2000) *EMBO J.* **19,** 5300–5307.
19. Din, N., Quardokus, E. M., Sackett, M. J. & Brun, Y. V. (1998) *Mol. Microbiol.* **27,** 1051–1063.
20. Yan, K., Pearce, K. H. & Payne, D. J. (2000) *Biochem. Biophys. Res. Commun.* **270,** 387–392.
21. Pla, J., Dopazo, A. & Vicente, M. (1990) *J. Bacteriol.* **172,** 5097–5102.
22. Sanchez, M., Valencia, A., Ferrandiz, M.-J., Sandler, C. & Vicente, M. (1994) *EMBO J.* **13,** 4919–4925.
23. Dai, K. & Lutkenhaus, J. (1992) *J. Bacteriol.* **174,** 6145–6151.
24. Dewar, S. J., Begg, K. J. & Donachie, W. D. (1992) *J. Bacteriol.* **174,** 6314–6316.
25. Feucht, A., Lucet, I., Yudkin, M. D. & Errington, J. (2001) *Mol. Microbiol.* **40,** 115–125.
26. Sambrook, J., Fritsch, E. F. & Maniatis, T. (1989) *Molecular Cloning: A Laboratory Manual* (Cold Spring Harbor Lab. Press, Plainview, NY), 2nd Ed.
27. Sun, Q. & Margolin, W. (2001) *J. Bacteriol.* **183,** 1413–1422.
28. Bi, E. & Lutkenhaus, J. (1990) *J. Bacteriol.* **172,** 2765–2768.
29. Guzman, L. M., Belin, D., Carson, M. J. & Beckwith, J. (1995) *J. Bacteriol.* **177,** 4121–4130.
30. Weiss, D. S., Chen, J. C., Ghigo, J. M., Boyd, D. & Beckwith, J. (1999) *J. Bacteriol.* **181,** 508–520.
31. Begg, K., Nikolaichik, Y., Crossland, N. & Donachie, W. D. (1998) *J. Bacteriol.* **180,** 881–884.
32. Ward, J. E. & Lutkenhaus, J. (1985) *Cell* **42,** 941–949.
33. Pichoff, S. & Lutkenhaus, J. (2001) *J. Bacteriol.* **183,** 6630–6635.
34. Hu, Z. & Lutkenhaus, J. (1999) *Mol. Microbiol.* **34,** 82–90.
35. Justice, S. S., Garcia-Lara, J. & Rothfield, L. I. (2000) *Mol. Microbiol.* **37,** 410–423.
36. van den Ent, F., Amos, L. A. & Lowe, J. (2001) *Nature* **413,** 39–44.
37. Yim, L., Vandenbussche, G., Mingorance, J., Rueda, S., Casanova, M., Ruysschaert, J. M. & Vicente, M. (2000) *J. Bacteriol.* **182,** 6366–6373.
38. Levin, P. A., Kurtser, I. G. & Grossman, A. D. (1999) *Proc. Natl. Acad. Sci. USA* **96,** 9642–9647.
39. Gueiros-Filho, F. J. & Losick, R. (2002) *Genes Dev.* **16,** 2544–2556.